Glucose Effectiveness Assessed under Dynamic and Steady State Conditions

Comparability of Uptake versus Production Components

Marilyn Ader, Ta-Chen Ni, and Richard N. Bergman

Department of Physiology and Biophysics, University of Southern California School of Medicine, Los Angeles, California 90033

Abstract

Glucose tolerance is determined by both insulin action and insulin-independent effects, or "glucose effectiveness," which includes glucose-mediated stimulation of glucose uptake (R_d) and suppression of hepatic glucose output (HGO). Despite its importance to tolerance, controversy surrounds accurate assessment of glucose effectiveness. Furthermore, the relative contributions of glucose's actions on R_d and HGO under steady state and dynamic conditions are unclear. We performed hyperglycemic clamps and intravenous glucose tolerance tests in eight normal dogs, and assessed glucose effectiveness by two independent methods. During clamps, glucose was raised to three successive 90-min hyperglycemic plateaus by variable labeled glucose infusion rate; glucose effectiveness (GE) was quantified as the slope of the dose-response relationship between steady state glucose and glucose infusion rate ($GE_{CLAMP(total)}$), R_d ($GE_{CLAMP(uptake)}$) or HGO ($GE_{CLAMP(HGO)}$). During intravenous glucose tolerance tests, tritiated glucose (1.2 μCi/kg) was injected with cold glucose (0.3 g/kg); glucose and tracer dynamics were analyzed using a two-compartment model of glucose kinetics to obtain R_d and HGO components of glucose effectiveness. All experiments were performed during somatostatin inhibition of islet secretion, and basal insulin and glucagon replacement. During clamps, R_d rose from basal (2.54±0.20) to 3.95±0.54, 6.76±1.21, and 9.48±1.27 mg/min per kg during stepwise hyperglycemia; conversely, HGO declined to 2.06±0.17, 1.17±0.19, and 0.52±0.33 mg/min per kg. Clamp-based glucose effectiveness was 0.0451±0.0061, 0.0337±0.0060, and 0.0102±0.0009 dl/min per kg for $GE_{CLAMP(total)}$, $GE_{CLAMP(uptake)}$, and $GE_{CLAMP(HGO)}$, respectively. Glucose's action on R_d dominated overall glucose effectiveness (72.2±3.3% of total), a result virtually identical to that obtained during intravenous glucose tolerance tests (71.6±6.1% of total). Both methods yielded similar estimates of glucose effectiveness. These results provide strong support that glucose effectiveness can be reliably estimated, and that glucose-stimulated R_d is the dominant component during both steady state and dynamic conditions. (*J. Clin. Invest.* 1997. 99:1187–1199.) Key words: glucose effectiveness • glucose turnover • dose response • mathematical modeling • intravenous glucose tolerance test

Introduction

Impaired glucose tolerance is a hallmark of the prediabetic state as well as full-blown non–insulin-dependent diabetes mellitus (NIDDM),[1] and is a risk factor for increased mortality due to cardiovascular disease (1). Normalization of glucose levels after oral or intravenous challenge depends on an adequate β-cell response to hyperglycemia, and sufficient insulin action to stimulate R_d and inhibit hepatic glucose output (HGO). An additional factor contributing to glucose tolerance is glucose effectiveness, defined as the action(s) of glucose per se, independent of increased insulin, to normalize glucose concentration through actions on glucose production and utilization (2, 3). Glucose effectiveness may contribute significantly to the efficient disposition of glucose, especially under conditions of reduced insulin action and prevailing hyperglycemia (4), and may be an independent risk factor for development of NIDDM (5).

Despite the apparent importance of glucose effectiveness to glucose tolerance, controversy surrounds the methods by which it is assessed. Quon et al. (6) have argued that minimal model–derived glucose effectiveness (S_G)[2] is overestimated, and they have suggested that the model attributes some of the effects of incremental insulin to the effects of glucose itself. Also, Finegood (7) has argued that reliable estimates for S_G are obtained only with a blunted insulin response. In contrast, Vicini and colleagues (8) have reported reliable estimates of overall S_G when a normal secretory profile was present. Thus, despite its importance to glucose tolerance in normal and pathologic states, there remains a fundamental uncertainty as to the proper methods for reliable estimation of S_G.

Given debate about measuring S_G, limited information is available about the physiologic mechanisms which determine glucose effectiveness. Specifically, while it is known that glucose can enhance glucose uptake (R_d) and inhibit HGO, the relative importance of these actions to glucose effectiveness is unclear. Glucose clamp studies done by Christopher et al. (9)

Address correspondence to Marilyn Ader, University of Southern California School of Medicine, Department of Physiology and Biophysics, MMR 624, 1333 San Pablo Street, Los Angeles, CA 90033. Phone: 213-342-1921; FAX: 213-342-1918; E-mail: ader@syntax.hsc.usc.edu

Received for publication 11 July 1996 and accepted in revised form 20 December 1996.

J. Clin. Invest.

0021-9738/97/03/1187/13 $2.00
Volume 99, Number 6, March 1997, 1187–1199

1. *Abbreviations used in this paper:* CV, coefficient of variation; GE, glucose effectiveness; GINF, glucose infusion rate; HGO, hepatic glucose output; IVGTT, intravenous glucose tolerance test; NIDDM, non–insulin-dependent diabetes mellitus; R_d, glucose uptake; S_G, minimal model-derived glucose effectiveness; SRIF, somatostatin.

2. Parameter S_G will be used only to refer to glucose effectiveness derived from minimal model analysis (or its modifications). Glucose effectiveness will be used to characterize the estimates obtained in this study from either the hyperglycemic clamp (GE_{CLAMP}) or the modified IVGTTS (GE_{IVGTT}) as described in this study.

indicate that at basal insulin, glucose effectiveness (= Δglucose infusion rate (GINF)/Δglucose) is dominated by the uptake component, which could be further dissected into nearly equal stimulation of glycogen synthesis and glycolysis. In contrast, Cobelli and his colleagues (8, 10) have measured S_G dynamically and reported that the uptake component accounts for only one-third of total glucose effectiveness, with the remainder accounted for by glucose's effect on HGO. No study has attempted to dissect the metabolic components of glucose effectiveness, comparing steady state clamps with dynamic intravenous glucose tolerance tests (IVGTT) in the same individuals. Therefore, the present study was designed to assess glucose effectiveness during both steady state and dynamic conditions, at fixed basal insulin, by two independent methodologies without using minimal model analysis. Additionally, under both conditions, we sought to determine the relative importance of glucose-stimulated R_d versus glucose-suppressed HGO on overall glucose effectiveness. Glucose effectiveness was assessed from clamps as the slope of the steady state relationship between glucose and glucose turnover. Also, we performed IVGTTs, in which tracer was injected along with cold glucose, and a two-compartment model of glucose kinetics was applied to both labeled and unlabeled glucose dynamics to dissect out the actions on R_d and HGO. Both methods yield similar estimates of glucose effectiveness, which are consistent with published minimal model values, providing strong support that glucose effectiveness can be reliably estimated. Furthermore, during both steady state conditions of the glucose clamp and after glucose injection, in normal animals, > 70% of glucose effectiveness is due to glucose's action on glucose uptake. The remaining component is due to glucose inhibition of HGO.

Methods

Animals

Experiments were performed on eight male mongrel dogs (mean: 25.8±1.0 kg) in the conscious, relaxed state. Animals were housed in the University of Southern California Vivarium under controlled kennel conditions (12 h light, 12 h dark) and fed standard chow (25% protein, 9% fat, and 49% carbohydrate: Wayne Dog Chow, Alfred Mills, Chicago, IL) once per day. Body temperature and weight were monitored regularly. Dogs were used for experiments only if judged healthy by general appearance and the above measurements. All procedures were approved by the University of Southern California Institutional Animal Care and Use Committee.

Surgical preparation

At least 7 d before the first experiment, surgery was performed as previously described (11) to implant indwelling catheters in the following vessels: (*a*) carotid artery, for blood sampling; (*b*) jugular vein, advanced into the right atrium, for glucose injection; (*c*) portal vein, for infusions of insulin and glucagon; and (*d*) femoral vein, for somatostatin (SRIF) infusion. All catheters were led subcutaneously to the back of the neck and exteriorized. Catheters were flushed with heparinized saline (100 U/ml) at regular intervals to maintain patency.

Experimental protocols

Each animal underwent two experiments to assess glucose effectiveness, during which the incremental β-cell response to glucose was blocked by SRIF: (*a*) multistep hyperglycemic clamp and (*b*) an IVGTT. Experiments were performed in random order, with at least 1 wk between experiments. All experiments were performed in overnight (15 h) fasted animals; during all tests, dogs were fully conscious, rested comfortably in a Pavlov sling, and were given free access to water.

Hyperglycemic clamps. On the morning of the clamp, one intracatheter was inserted in the saphenous vein for infusion of glucose; a urinary catheter was also inserted for urine collection to account for glycosuria when plasma glycemia exceeded the renal threshold. Three basal arterial samples were collected at $t = -80$, -70, and -61 min. At $t = -60$ min, systemic infusion of SRIF was begun (0.8 μg/min per kg, $n = 3$; 1.6 μg/min per kg, $n = 5$), along with intraportal infusions to replace endogenous insulin (0.2 mU/min per kg) and glucagon (0.65 ng/min per kg). (The higher dose of SRIF was used after we observed early evidence of insulin breakthrough during severe hyperglycemia [∼ 500 mg/dl; data not used] when using the lower infusion rate.) Blood sampling was continued at 10-min intervals for 60 min ("basal replacement period") to assess the effect of the basal replacement regimen on glycemia and hormone levels.

At time 0, a three-step hyperglycemic clamp was initiated (target glucose: 150, 225, and 300 mg/dl), with exogenous glucose spiked with tritiated glucose (desired specific activity of infusate: 2.7 μCi/g; upon assay: 2.53±0.03 μCi/g) to avoid large fluctuations in plasma specific activity. Blood samples were drawn every 5 min for the first 30 min, and glucose infusion adjusted manually to achieve target glycemia. From $t = 30$–90 min, samples were drawn at 10-min intervals, after which rapid sampling was repeated beginning at $t = 90$ min to facilitate attainment of the second hyperglycemic plateau. At $t = 180$ min, the third hyperglycemic level was begun and continued to 270 min. Samples were assayed for glucose (on-line), insulin, FFA, and [^{3}H]glucose. Additional 3-ml samples were drawn at the following times for determination of plasma glucagon: $t = -80$, -61, -20, -1, 60, 90, 150, 180, 240, and 270 min. A total of 36 blood samples were drawn during the clamp. Urine was collected at 10-min intervals from 0 to 270 min, total volume recorded, and an aliquot removed and stored at 20°C for subsequent assay of glucose.

Intravenous glucose tolerance test. Three basal arterial samples were collected at $t = -80$, -70, and -61 min. At $t = -60$ min, systemic infusions of SRIF with intraportal insulin and glucagon were initiated. Blood sampling was continued as described for hyperglycemic clamps. At time 0, glucose (0.3 g/kg), with added tracer (desired: 1.2 μCi/kg; upon assay: 1.08±0.01 μCi/kg) was injected over 30 s via the right atrial catheter, and blood samples were drawn at 2, 3, 4, and 5 min, every 2 min from 6 to 16 min, every 3 min from 19 to 25 min, every 10 min from 30 to 120 min, and at 140, 160, and 180 min. These samples were assayed for glucose, insulin, and [^{3}H]glucose. An additional 3 ml were drawn at the following times for determination of plasma glucagon: $t = -80$, -61, -20, -1, 140, 160, and 180 min. A total of 35 blood samples were drawn during the IVGTT.

Control experiments

To account for possible time-dependent changes in glucose, glucose turnover, and other measured variables during the 360-min hyperglycemic clamp, we performed a series of experiments on an additional set of dogs ($n = 3$). In these studies, tracer, SRIF, insulin, and glucagon were administered as described for hyperglycemic clamps (glucagon infusion rate: 0.65 ng/min per kg), but no exogenous glucose was infused.

Blood sampling

Blood samples were collected in tubes containing heparin and NaF and stored on ice until centrifugation. Samples for FFA determination were collected in tubes containing paraoxan and EDTA, and samples for glucagon assay were collected into chilled tubes containing Trasylol (aprotinin, 500 U/ml blood; FBA Pharmaceuticals, New York) as well as heparin/NaF mixture. After separation, samples were stored at −20°C until assayed for glucose, insulin, FFA, and [^{3}H]glucose, or at −70°C until assayed for glucagon.

Assays

Plasma glucose was assayed in duplicate by the glucose oxidase technique on an automated analyzer (model 23A, Yellow Springs Instru-

ments, Yellow Springs, OH). Intraassay coefficient of variation (CV) of the glucose assay was ±1%. Urine glucose was assayed in duplicate with the STATZYME colorimetric assay (Sigma Chemical Co., St. Louis, MO). Plasma insulin was measured in duplicate by the highly specific sandwich ELISA (12), rather than the polyclonal antibody radioimmunoassay which is known to cross-react to varying degrees with proinsulin and insulin split products. The ELISA uses two murine mAbs which bind to distinct epitopes on the insulin molecule; antibody HUI-018 binds to the A-chain, and antibody OXI-005 targets the COOH terminus of the B-chain. The insulin assay was established in our laboratory with the kind assistance of B. Dinesin of Novo-Nordisk (Copenhagen, Denmark). Limit of detection in the ELISA is 5 pM, with intra- and interassay CV of 3±1% and 5±1%, respectively.

For the determination of [3-^{3}H]glucose, samples were deproteinized with Zn_2SO_4 and $BaOH_2$ (13). The supernatant was then dried at 70°C, redissolved in water, and counted in ReadySafe scintillation fluid (Beckman Instruments Inc., Fullerton, CA) on a liquid scintillation counter (Beckman Instruments, Inc.) with a two-channel dual-label automatic quench correction program. Glucagon was assayed from plasma by radioimmunoassay with minimal cross-reactivity to enteric glucagon (< 0.1%). Because of technical difficulties, glucagon assays were only performed on a subset of IVGTT experiments (n = 3). Glucagon was assayed from control experiments with the LINCO assay, run against standards provided by Novo-Nordisk (intra-assay CV: 6±1%).

Materials

Cyclic somatostatin was purchased from Bachem, California (Torrance, CA). Insulin (regular purified pork for injection) was purchased from Novo-Nordisk, and glucagon (purified pork) was purchased from Sigma Chemical Co. HPLC-purified d-[3-^{3}H]glucose was bought from Dupont-NEN (Boston, MA). Dextrose (50%) was purchased from Kendall McGaw (Irvine, CA). Murine mAbs and the canine insulin standard for ELISA were kindly donated by B. Dinesen of Novo-Nordisk.

Calculation of glucose effectiveness

Hyperglycemic clamps. Glucose effectiveness represents the combined actions of hyperglycemia, independent of an increase in insulin, to accelerate R_d and inhibit HGO. During hyperglycemic clamps in which β-cell secretion is blocked by SRIF, and insulin is replaced, the amount of glucose infused to attain each of the three hyperglycemic plateaus represents the combined actions of hyperglycemia per se on R_d and HGO at each glucose level. Thus, total glucose effectiveness (GE) from the clamp ($GE_{CLAMP(total)}$) was estimated for each animal as the slope of the relationship between steady state glucose and glucose infusion rate, assuming the relationship is linear (see Results). Similarly, the component of glucose effectiveness describing the stimulatory effects of hyperglycemia on R_d ($GE_{CLAMP(uptake)}$) was calculated for each dog as the slope of glucose versus R_d, after correction for urinary loss. Finally, the actions of hyperglycemia to inhibit HGO ($GE_{CLAMP(HGO)}$) was calculated as the absolute value of the (negative) slope of glucose versus HGO during the clamp.

IVGTTs

Compartmental analysis. To quantify glucose effectiveness from the IVGTT, and to distinguish and quantify the distinct effects of glucose on R_d and HGO, we used the simplest mathematical model that could adequately describe dynamics of labeled and unlabeled glucose after injection. Model development is described in detail (see Appendix). The model for simultaneous assessment of glucose's actions on R_d and HGO during the IVGTT is the two-compartment representation shown in Fig. 1.

Compartment 1 ("fast compartment") consists of plasma and tissues that equilibrate rapidly with plasma. This compartment presumably includes plasma water, the interstitial space of liver, spleen, and bone marrow, the central nervous system, and interstitial space of the endocrine and splanchnic organs (14). Compartment 2 represents the

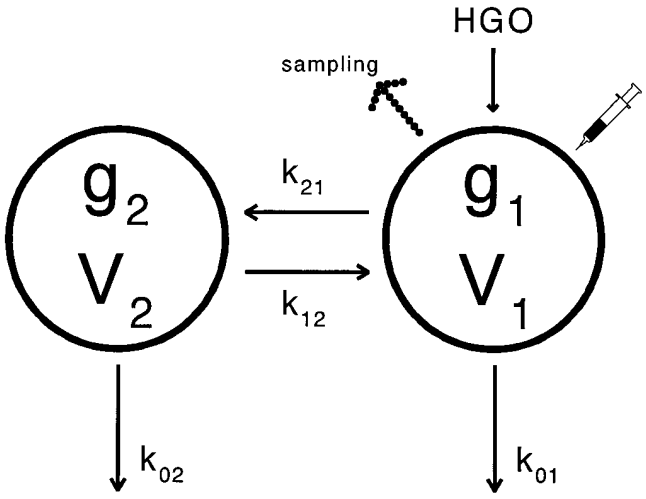

Figure 1. Two-compartment model of glucose kinetics. Compartment 1 represents the accessible (plasma) pool, into which glucose and tracer are injected, and HGO enters. Glucose disappearance from this compartment is considered to be independent of insulin, and includes uptake by tissues such as central nervous system and liver. The second compartment represents the remote, interstitial compartment, and is considered the primary site of insulin-stimulated glucose uptake.

pool that equilibrates slowly with plasma ("slow compartment"), presumably including the interstitial space of striated muscle, adipose tissue, and smooth muscle of some organs (14). It has been suggested that glucose uptake from compartment 1 is non–insulin mediated, whereas uptake from the second compartment is sensitive to insulin (15). This model is characterized by the following equations:

For unlabeled glucose:

$$\frac{dq_1(t)}{dt} = HGO(t) + k_{12}q_2(t) - [k_{01} + k_{21}]\,q_1(t); q_1(0) = q_{10} \quad (1a)$$

$$\frac{dq_2(t)}{dt} = k_{21}q_1(t) - [k_{02} + k_{12}]\,q_2(t); q_2(0) = q_{20} \quad (1b)$$

$$g_1(t) = \frac{q_1(t)}{V_1} \quad (1c)$$

where q_1 and q_2 are the masses of unlabeled glucose in compartments 1 and 2, respectively. Variable g_1 is the concentration of unlabeled glucose in compartment 1, and V_1 represents the distribution volume of that compartment. Kinetic parameters (k_{ij}'s) represent fractional transfer or disappearance rate constants between compartments. HGO is hepatic glucose output, which is time dependent during the IVGTT.

Similarly, for labeled glucose:

$$\frac{dq_1^*(t)}{dt} = k_{12}q_2^*(t) - [k_{01} + k_{21}]q_1^*(t);\ q_1^*(0) = DOSE^*_{Total} \quad (2a)$$

$$\frac{dq_2^*(t)}{dt} = k_{21}q_1^*(t) - [k_{02} + k_{12}]\,q_2^*(t); q_2^*(0) = 0 \quad (2b)$$

$$g_1^*(t) = \frac{q_1^*(t)}{V_1} \quad (2c)$$

where q_1^* and q_2^* are the tracer masses in compartments 1 and 2, respectively, and variable g_1^* is the concentration of labeled glucose in compartment 1. $DOSE^*_{Total}$ is the total dose of labeled glucose injected at time 0. All the kinetic parameters in Eqs. 2a and 2b (k_{01}, k_{02}, k_{21} and k_{12}) are assumed to be equivalent to those in Eqs. 1a and 1b,

i.e., we assume no isotope discrimination under the conditions of these experiments.

Since the parameters of this model cannot be estimated a priori from a single IVGTT (16), one additional assumption is necessary to identify the model. In this study, we assumed uptake from the insulin-sensitive second compartment to be negligible, i.e., $k_{02} = 0$ (17, 18). While this assumption can be scrutinized, modeling demonstrated that the calculation of relative contributions of R_d versus HGO to glucose effectiveness is independent of the value of k_{02} (see Appendix).

Since labeled glucose is not produced in vivo, tracer dynamics are affected by glucose disappearance only, while unlabeled glucose dynamics are affected by both HGO and R_d. As a result, Eqs. 2a and 2b have fewer parameters than Eqs. 1a and 1b. The strategy to identify the full model for both unlabeled and labeled glucose dynamics is as follows. First, we fit Eqs. 2a, 2b, and 2c to labeled glucose dynamics to determine k_{01}, k_{12}, k_{21}, and the distribution volume (V_1). Unlabeled glucose dynamics were then used to determine the kinetics of hepatic glucose output. Given that HGO is believed to be negatively correlated with plasma glucose concentration during glucose clamps (see Results) or the IVGTT (19), the relationship between HGO and glucose mass in plasma (q_1) was represented by the following relation:

$$HGO(t) = HGO_0 - k_L \times q_1(t) \quad (3)$$

where HGO_0 is the extrapolated rate of glucose production as plasma glucose mass approaches zero, and k_L is the parameter describing the effect of plasma glucose on HGO. Eqs. 1a, 1b, and 1c were used to fit unlabeled glucose dynamics to determine the initial glucose concentration (g_{10}) and k_L.

Definition of glucose effectiveness from the model. The uptake component of glucose effectiveness ($GE_{IVGTT(uptake)}$) is the increase of R_d per unit increase of glucose at basal insulin, independent of an insulin response.[3] The elevation in glycemia will increase R_d and consequently accelerate the normalization of the plasma glucose. Similarly, the HGO component of glucose effectiveness is the decrease of HGO per unit increase of glucose, again at basal insulin; this reduction in HGO will also aid in the normalization of plasma glucose after a glucose load. $GE_{IVGTT(uptake)}$ was determined from labeled glucose dynamics which reflect only the kinetics of R_d, while $GE_{IVGTT(HGO)}$ was determined from the dynamics of cold glucose, which reflect both uptake and production. The peripheral component of glucose effectiveness is defined as follows:

$$GE_{1VGTT(uptake)} = \frac{\Delta(R_d)^{Total}}{\Delta(Glucose\ mass)^{Accessible\ Pool}} = \frac{\Delta(k_{01}q_1^* + k_{02}q_2^*)}{\Delta(q_1^*)} = k_{01} \text{ if } k_{02} = 0. \quad (4)$$

The component of glucose effectiveness which describes glucose's actions to suppress HGO is defined as follows:

$$GE_{1VGTT(HGO)} = \frac{-\Delta(HGO)^{Total}}{\Delta(Glucose\ mass)^{Accessible\ Pool}} = \frac{-\Delta(HGO)^{Total}}{\Delta(q_1)} = k_L. \quad (5)$$

Data analysis and calculations

Steady state during clamps was defined as the final 30 min of each period.[4] From IVGTT data, glucose tolerance (K_G) was calculated as the negative slope of the natural log of glucose versus time from 10 to 40 min. Glucose-stimulated first-phase insulin release was calculated as the integrated plasma insulin response above preinjection levels from 0 to 10 min. Modeling analysis was carried out by MLAB implemented on an IBM-compatible computer (Civilized Software, Bethesda, MD). Parameters of all compartmental models were identified by weighted nonlinear least-squares fitting using a Marquardt-Levenburg algorithm with inverse variance weights.

All statistics (t tests and ANOVA) were performed using MINITAB statistical software. Data are reported as mean±SE. Statistical significance was set at $P \leq 0.05$.

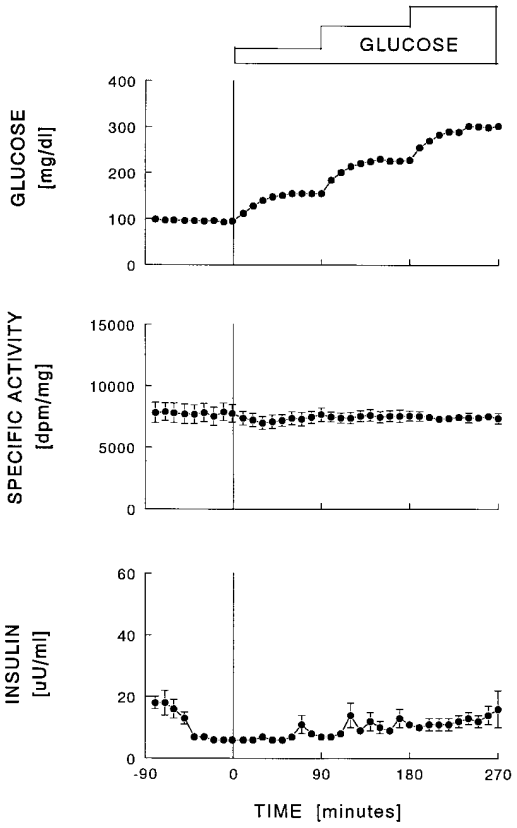

Figure 2. Time course of glucose, specific activity, and insulin during hyperglycemic clamps. Somatostatin, with intraportal insulin and glucagon, was infused from $t = -60$ to 270 min.

Results

Basal replacement

During hyperglycemic clamps, basal glucose averaged 98±1 mg/dl (Table I), and remained stable despite insulin underreplacement (7±1 vs 18±3 μU/ml; $P = 0.003$). Plasma FFA and lactate were unchanged during the basal replacement period.

Before the IVGTTs, glucose rose modestly from basal (109±6 vs 96±2 mg/dl; $P = 0.053$) because of insulin underreplacement (7±1 vs 16±2 μU/ml; $P = 0.0009$), since glucagon was unchanged during this period (Table I). Despite modestly

3. Alternatively, glucose effectiveness can be defined relative to the size of the glucose pool (compartments 1 and 2) rather than to the accessible (= plasma) glucose pool only. However, to facilitate comparison of our estimates of glucose effectiveness with those of other models (10, 51), including clamps in which only plasma measurements are available, we have chosen to define glucose effectiveness from the two-compartment model relative to the size of compartment 1 only.

4. Since glucose infusion rates were abruptly increased at $t = 90$ and 180 min to rapidly achieve hyperglycemic levels, steady state for glucose infusion and turnover rates was calculated from 60–80 min, 150–170 min, and 240–260 min.

Table I. Plasma Metabolite and Hormone Concentrations during Clamps and IVGTTs

	Basal*	SRIF	SS-1	SS-2	SS-3
Hyperglycemic clamps					
Glucose‡	98±1	95±3	155±3	228±4	302±4
Insulin	18±3	7±1	8±1	11±2	14±2
Glucagon§	—	—	—	—	—
FFA	0.46±0.07	0.44±0.06	0.31±0.05	0.18±0.03	0.13±0.03
Lactate	5.45±1.43	5.32±1.05	8.41±1.52	10.27±1.51	10.81±1.94
Control experiments‖					
Glucose	93±2	85±5	74±6	69±4	63±1
Insulin	14±3	7±1	6±1	7±1	6±1
Glucagon	89±15	66±5	63±6	65±4	74±3
FFA	0.90±0.28	0.82±0.25	0.83±0.22	0.72±0.25	0.63±0.14
Lactate	4.76±0.90	5.79±1.12	7.44±1.72	9.57±3.98	9.94±4.44
IVGTTs					
Glucose	96±2	109±6	—	—	—
Insulin	16±2	7±1	—	—	—
Glucagon	(35±3)	(38±8)	—	—	—

*Basal denotes mean of samples drawn before initiation of combined SRIF, insulin, and glucagon infusions. SRIF represents mean of samples drawn at −20, −10, −1 min, before initiation of experiment at $t = 0$ min. SS-1, SS-2, and SS-3 represent steady state target glycemia of 150, 225, and 300 mg/dl during hyperglycemic clamps. ‡Units are as follows: glucose, mg/dl; insulin, μU/ml; glucagon, pg/ml; FFA, mmol/liter; lactate, mg/dl. §Glucagon values are only available for IVGTTs performed on three dogs (see Methods). ‖Control experiments are identical to hyperglycemic clamps, except no glucose is infused (see Methods).

higher glucose during this period compared with basal, glucose levels were stable before glucose injection at time 0 (CV (−20 to −1 min) = ±3%). Plasma insulin remained stable for ≥ 40 min before the initiation of hyperglycemia during both clamps and IVGTTs.

Hyperglycemic clamp

Glucose and glucose infusion rates. Plasma glucose attained levels of 155±3, 227±4, and 301±4 mg/dl within ~ 40 min of the start of each hyperglycemic phase; levels were stable during the final 30 min of each period (CV: 4±1, 4±1, and 3±1%, respectively: Fig. 2). Despite high dose SRIF (1.6 μg/min per kg), we observed small increments in plasma insulin with increasing glucose (8±1, 11±2, and 14±2 μU/ml; $P = 0.008$), although concentrations remained below ambient, pre-SRIF levels (18±3 μU/ml). Stepwise hyperglycemia resulted in a progressive decrease in plasma FFA ($P < 0.0001$ by ANOVA), while plasma lactate levels increased ($P < 0.001$ by ANOVA; Table I). Changes in FFA and lactate may be due in part to a time effect or the actions of SRIF per se (20) (see below).

In the absence of infused glucose, infusions of SRIF, insulin, and glucagon caused a steady decline in glucose because of prolongation of the fasted state (Table I). This occurred despite an insulin underreplacement (7±1 vs 14±3 μU/ml; $P < 0.001$) of similar degree as observed in hyperglycemic clamps. Glucagon was slightly, but not significantly underreplaced (66±5 vs 89±15 pg/ml; $P = 0.18$), and remained stable for the entire experimental period. Despite insulin underreplacement, FFA exhibited a tendency to decline over time (Table I), although neither this trend nor the upward trend in lactate was statistically significant ($P = 0.505$ and 0.333, respectively, by ANOVA).

During hyperglycemic clamps, glucose infusion rates required to attain each level of hyperglycemia were 2.09±0.62, 5.60±0.96, and 9.42±1.32 mg/min per kg (C.V.: 18±9, 10±5, and 13±4%; Table II). Since exogenously infused glucose was spiked with [^{3}H]glucose, plasma specific activity remained stable throughout the clamp (Fig. 2).

Dose response effects of stepwise hyperglycemia on glucose turnover. Glucose uptake tended to decrease slightly during

Table II. Glucose Infusion Rates and Glucose Turnover during Hyperglycemic Clamps

	Basal	SRIF	SS-1	SS-2	SS-3
Hyperglycemic clamps					
Glucose infusion*	—	—	2.09±0.62	5.60±0.96	9.42±1.32
R_d	2.54±0.20	2.35±0.27	3.95±0.54	6.76±1.21	9.48±1.27
HGO	2.54±0.20	2.68±0.15	2.06±0.17	1.17±0.19	0.52±0.33
Control experiments‡					
Glucose infusion	—	—	—	—	—
R_d	2.25±0.02	2.36±0.08	2.15±0.04	2.42±0.24	2.52±0.30
HGO	2.25±0.02	2.12±0.20	2.07±0.04	2.29±0.20	2.43±0.27

*Data are expressed in milligrams per minute per kilogram. ‡Control experiments were performed as described in Table I and Methods.

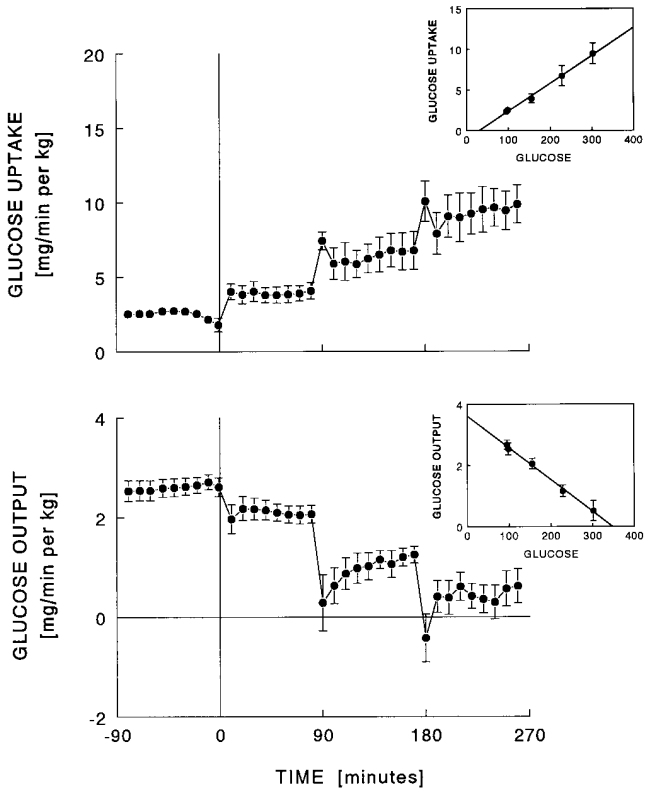

Figure 3. Time course of glucose uptake and HGO during hyperglycemic clamps. Note the rapid attainment of stable R_d and HGO within each 90-min hyperglycemic period. Insets reveal the strong linear dose response relationship between glucose and both R_d (*top*) and HGO (*bottom*) at steady state.

the basal replacement period (2.35±0.27 vs 2.54±0.20 mg/min per kg; $P = 0.2$). Hyperglycemia caused a rapid, dose-dependent increase in R_d (Table II), in which uptake rates within 10% of steady state values were attained within 20–40 min of hyperglycemia (Fig. 3). Similar rapid dynamics were observed for hyperglycemia-mediated suppression of HGO, i.e., hepatic glucose autoregulation (Fig. 3). After a slight increase in HGO during the basal replacement period (2.68±0.15 vs 2.54±0.20 mg/min per kg; $P = 0.23$), HGO exhibited a dose-dependent decrease during progressive hyperglycemia (Table II).

There were no time-dependent changes observed in either HGO ($P = 0.472$) or glucose utilization ($P = 0.468$) during control experiments (Table II).

Linearity of the glucose dose response relationship. The relationship between glucose and both R_d and HGO was linear throughout the range of glucose examined (mean *r* value, vs R_d: 0.970±0.008, range: 0.937–0.995; mean, vs HGO: 0.959±0.014, range: 0.869–0.993; Fig. 3, *insets*). Furthermore, in the relationship between glucose and R_d, we observed no positive intercept on the ordinate, in contrast to previous reports (e.g., 21, 22). The explanation for this discrepancy may be because of differences in tracer methods used for assessment of glucose uptake (see Discussion).

Glucose effectiveness from the hyperglycemic clamp. The combined actions of hyperglycemia to increase R_d and suppress HGO independent of elevated insulin levels were quantified from hyperglycemic clamps as total glucose effectiveness, or

Table III. Individual Values of Total Glucose Effectiveness, and Its Uptake and HGO Components, Calculated from Hyperglycemic Clamps for Each Animal

Dog	$GE_{CLAMP\ (total)}$	$GE_{CLAMP\ (uptake)}$		$GE_{CLAMP\ (HGO)}$	
	dl/min per kg	*dl/min per kg*	*% Total*	*dl/min per kg*	*% Total*
1	0.0387	0.0258	66.67	0.0116	29.97
2	0.0715	0.0639	89.37	0.0083	11.61
3	0.0303	0.0189	62.38	0.0084	27.72
4	0.0355	0.0275	77.46	0.0077	21.69
5	0.0597	0.0420	70.28	0.0157	26.30
6	0.0642	0.0512	79.75	0.0110	17.13
7	0.0351	0.0239	68.09	0.0089	25.36
8	0.0256	0.0162	63.28	0.0098	38.28
Mean	0.0451	0.0337	72.16	0.0102	24.76
SE	0.0061	0.0060	3.29	0.0009	2.87

Glucose effectiveness was calculated from hyperglycemic clamps as the slope of the relationship between steady state glucose and glucose infusion rate ($GE_{CLAMP(total)}$), R_d($GE_{CLAMP(uptake)}$), or HGO ($GE_{CLAMP(HGO)}$).

$GE_{CLAMP(total)}$. This parameter averaged 0.0451±0.0061 dl/min per kg (Table III), but exhibited a nearly threefold range across this sample of normal dogs. The uptake component of clamp-based glucose effectiveness ($GE_{CLAMP(uptake)}$) averaged 0.0337±0.0060 dl/min per kg, (range: 0.0162–0.0639) and dominated total glucose effectiveness (72.2±3.3% of $GE_{CLAMP(total)}$). Hyperglycemia-mediated suppression of HGO ($GE_{CLAMP(HGO)}$) represented a quantitatively smaller component of total glucose effectiveness (0.0102±0.0009 dl/min per kg; 24.8±2.9% of $GE_{CLAMP(total)}$), but may contribute as much as 38% to total glucose effectiveness in some animals (compare dog 8).

Intravenous glucose tolerance test

Glucose peaked at 299±10 mg/dl within 2 min. With SRIF, the acute insulin response was not different from zero (5.9±3.4 μU/ml per 10 min; $P = 0.13$; Table IV). Total glucose-stimulated insulin response was mostly blocked by SRIF (incremen-

Table IV. Glucose-stimulated Insulin Release and Glucose Tolerance during IVGTTs with Somatostatin Infusion

Dog	Integrated insulin*		K_G‡
	Acute	Total	
1	2	638.5	1.11
2	22.5	253.5	0.77
3	7.5	−11.5	0.87
4	2	169	0.41
5	−1.5	−43.5	1.17
6	18.5	165	0.76
7	1	65	0.73
8	−4.5	−35	1.21
Mean±SE	5.9±3.4§	150.1±79.6§	0.88±0.10

*Integrated insulin is defined as area above preinjection insulin from 0–10 min (acute) or 0–180 min (total), in units of μU/ml. ‡Glucose tolerance is defined by the K_G, the negative slope of the natural log of glucose versus time from 10 to 40 min. Units of K_G are percent/min^{-1}. §Not statistically different from zero ($P > 0.1$).

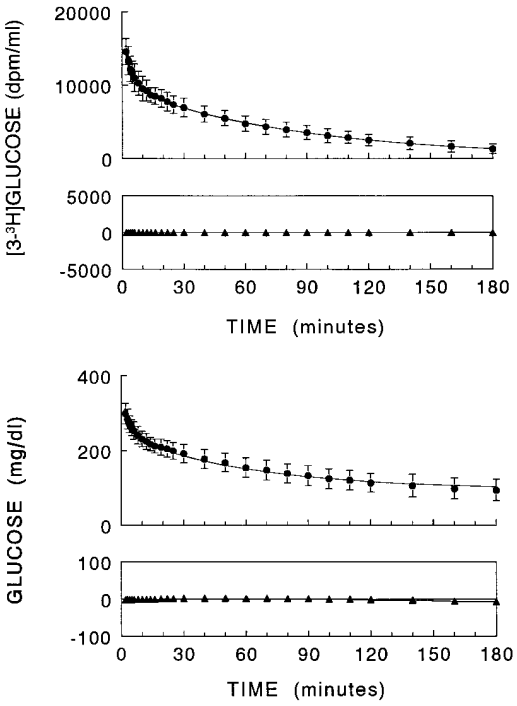

Figure 4. Model fit of (*top*) labeled and (*bottom*) unlabeled glucose, with corresponding residuals, during the IVGTT. Symbols represent average data ($n = 8$), and solid line the average fit with standard error. Residuals are calculated at each data point as the difference between experiment data and model fit.

tal insulin: 150.1±79.6 μU/ml per 180 min; $P = 0.10$ vs zero). In the absence of a significant dynamic insulin response, glucose tolerance was impaired (K_G=0.88 %/min^{-1}), although glucose was renormalized by the end of the test. After an initial rapid phase, tracer concentration steadily declined, but was still above zero at 180 min (1352±241 dpm/ml; $P = 0.0009$).

Two-compartment model results. The two-compartment model in Fig. 1 was applied to the labeled and unlabeled IVGTT data collected from each animal. Overall precision in parameter estimates was satisfactory (Table V), with mean fractional SD ranging from 4.8 to 21.7%. Among kinetic parameters, k_{01} averaged 0.0267±0.0014 min^{-1}. Parameters k_{21} and k_{12} averaged 0.111±0.023 and 0.123±0.029 min^{-1}, respectively. These parameters, which represent the distribution kinetics between the fast and slow compartments, were an order of magnitude larger than the disappearance parameter, k_{01}. The effect of glucose on HGO (parameter k_L) averaged 0.0092±0.0024 min^{-1}. Mean distribution volume of the first compartment (V_1) was 3.32±0.23 liters. Average model fits, with residuals, for both labeled and unlabeled glucose are shown in Fig. 4. The two-compartment model described both labeled and unlabeled glucose kinetics satisfactorily over the entire experimental duration, with no significant residual runs. Only a slight deviation of the model fit to raw data was observed for unlabeled glucose at the end of the experiment.

Dissection of glucose effectiveness from the IVGTT. From two-compartment analysis of labeled and unlabeled glucose dynamics during the IVGTT, we obtained quantitative estimates in each animal of the contribution of glucose-stimulated glucose uptake ($GE_{IVGTT(uptake)}$) and glucose-mediated suppression of HGO ($GE_{IVGTT(HGO)}$) to overall glucose effectiveness (Table VI). Overall, $GE_{IVGTT(uptake)}$ was over twofold higher than $GE_{IVGTT(HGO)}$ (0.0206±0.0014 vs 0.0092±0.0024 min^{-1}), and constituted the dominant component of total glucose effectiveness from the IVGTT (71.6±6.1 vs 28.4±6.1%).

Comparison of glucose effectiveness from the clamp and IVGTT

The relative contribution of the effects of hyperglycemia per se on R_d and HGO from the hyperglycemic clamps and IVGTT are compared in Fig. 5. The relative contributions of uptake versus HGO effects were remarkably similar between the two independent approaches. Hyperglycemia-mediated stimulation of R_d comprised 72.2±3.3% and 71.6±6.1% of total glucose effectiveness from the clamp and IVGTT, respectively (P =

Table V. Individual Kinetic Parameters of the Two-Compartment Model Identified from Both Labeled and Unlabeled Glucose Data from the IVGTT

	Kinetic parameters			Distribution volume	HGO sensitivity
Dog	k_{01}*	k_{21}	k_{12}	V_1	k_L
1	0.0276	0.1051	0.1419	45.3	0.00474
2	0.0177	0.0879	0.1408	34.2	0.00248
3	0.0207	0.1632	0.1892	24.9	0.01191
4	0.0212	0.2466	0.2542	28.4	0.00482
5	0.0212	0.0669	0.0111	27.7	0.01974
6	0.0216	0.0768	0.0121	33.7	0.00383
7	0.0139	0.0669	0.0978	38.6	0.01896
8	0.0212	0.0702	0.1357	32.8	0.00689
Mean	0.0206	0.1105	0.1229	33.2	0.00917
SE	0.00137	0.0225	0.0292	2.3	0.00244
% FSD‡	5.59±1.89	16.68±4.07	9.67±1.21	4.79±1.88	21.68±4.61

*All parameters are in units of min^{-1}; distribution volumes are expressed in deciliters. ‡The percent fractional standard deviation (% FSD) is defined as: $100 * \frac{SD\ of\ parameter\ estimate}{parameter\ estimate}$.

Table VI. Individual Values of $GE_{IVGTT(uptake)}$ and $GE_{IVGTT(HGO)}$ Obtained by Two-Compartment Analysis of IVGTTs for Each Animal

	$GE_{IVGTT\ (total)}$	$GE_{IVGTT\ (uptake)}$		$GE_{IVGTT\ (HGO)}$	
Dog	min^{-1}	min^{-1}	% Total	min^{-1}	% Total
1	0.0323	0.0276	85.34	0.0047	14.66
2	0.0202	0.0177	87.72	0.0025	12.28
3	0.0326	0.0207	63.49	0.0119	36.51
4	0.0260	0.0212	81.53	0.0048	18.47
5	0.0409	0.0212	51.75	0.0197	48.25
6	0.0254	0.0216	84.94	0.0038	15.06
7	0.0329	0.0139	42.36	0.0190	57.64
8	0.0281	0.0212	75.49	0.0069	24.51
Mean	0.0298	0.0206	71.58	0.0092	28.42
SE	0.0022	0.0014	6.06	0.0024	6.06

$GE_{IVGTT\ (uptake)}$ and $GE_{IVGTT\ (HGO)}$ are estimated from simultaneous analysis of labeled and unlabeled glucose after injection (see Methods). $GE_{IVGTT\ (total)}$ is the arithmetic sum of the two components.

0.97), and glucose-mediated inhibition of HGO comprised 24.8±2.9% of total glucose effectiveness in the clamp, and 28.4±6.1% during IVGTTs performed in the absence of incremental insulin. While it may well have been of interest to compare these independent measures of glucose effectiveness among the individual animals, because of the limited range of glucose effectiveness, a strong correlation between these variables cannot be expected, even if both methods measured effectiveness accurately (see Discussion).

Discussion

Glucose effectiveness is a little understood factor in the regulation of glucose tolerance, the importance of which is becoming increasingly appreciated. While insulin sensitivity can be easily manipulated by pharmacologic or physical interventions, glucose effectiveness is similar in many different metabolic states (23), although it may be reduced in NIDDM (24). In fact, Martin et al. (5) reported that decreased minimal model–derived glucose effectiveness (parameter S_G) was an independent risk factor for development of NIDDM in offspring of two diabetic parents. Henriksen and his colleagues (25) observed higher S_G in another group of high risk individuals. Furthermore, in NIDDM, the importance of glucose effectiveness to glucose tolerance may be substantial. Insulin secretion is suppressed (26), and insulin resistance is usually profound, such that within the physiologic concentration range insulin has little measurable effect to increase R_d (27, 28). Thus it follows that glucose effectiveness is the primary determinant of R_d in the type 2 diabetic state (29), as confirmed by Alzaid and colleagues (27) from meal tolerance studies in which glucose balance across muscle bed were assessed. Even without diabetes, glucose effectiveness is important to glucose normalization after a carbohydrate challenge (29).

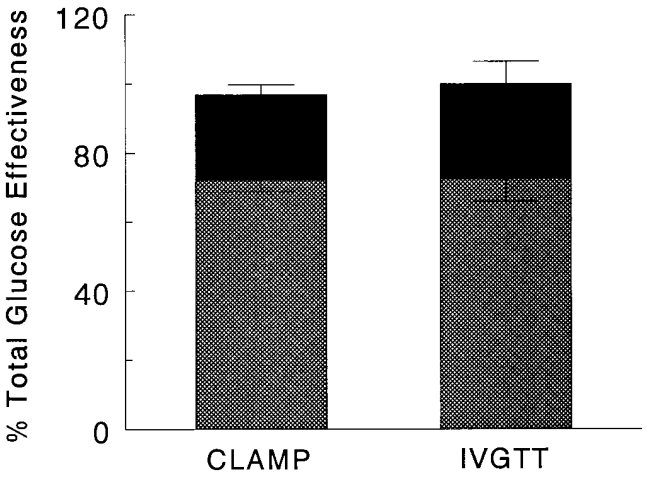

Figure 5. Dissection of glucose effectiveness calculated from the hyperglycemic clamp or IVGTT into uptake (*hatched bars*) and HGO (*solid bars*) components. Despite widely varying methodologies and methods of analysis, the relative contribution of glucose-stimulated glucose uptake ($GE_{(uptake)}$) to total glucose effectiveness was nearly identical between protocols (72.2 vs 71.6%).

Despite its importance to glucose tolerance, controversy exists as to methods for accurate assessment of glucose effectiveness. Finegood et al. (7) assert that accurate estimation from the minimal model is possible only if insulin secretion is suppressed, while Vicini and colleagues (8) have not observed any interference by secreted insulin. Quon et al. (6) argue that S_G is overestimated by the minimal model, while insulin sensitivity is underestimated. Christopher et al. (9) performed elegant studies to assess glucose effectiveness under steady state conditions of the glucose clamp, but did not examine the dynamic state. The present study was designed to help clarify these different approaches by quantifying glucose effectiveness under both steady state and dynamic conditions, using two independent methods—one dynamic and one steady state. We also examined the partitioning of glucose effectiveness into its actions on R_d and HGO under both conditions. Our results indicate that glucose effectiveness measured during the hyperglycemic clamp and IVGTT at near-basal insulin are similar, and consistent with published minimal model estimates. Furthermore, partitioning of glucose effectiveness was nearly identical in clamps and the IVGTT: 72% stimulation of R_d and 28% suppression of HGO, thus providing convincing support for the physiologic processes underlying glucose effectiveness under both conditions.

Our results by two independent methods confirm the results of Christopher et al. (9) that the ability of glucose to accelerate R_d is the dominant action of glucose to effect its own normalization, accounting for nearly 72% of glucose effectiveness. Christopher et al. (9) reported that 79% of glucose effectiveness at basal insulin was due to the actions of glucose per se on R_d. The present study extends the work of Christopher in two major ways. First, in the present study, all clamps were performed at three levels of hyperglycemia (150, 225, and 300 mg/dl). This more complete dose response study enabled us to verify the linearity of glucose's actions on both R_d and HGO, thus avoiding unnecessary assumptions; glucose effectiveness could then be reliably calculated as the slope of this linear relationship. More important, this study is the first to dissect the relative contributions of R_d versus HGO to glucose effectiveness during both steady state and dynamic conditions in a single set of individuals. Despite completely independent methods of analysis for clamps and IVGTTs, the partitioning of glucose effectiveness was remarkably similar (Fig. 5), with glu-

cose's actions on R_d accounting for an average of 72% of the overall parameter value, regardless of whether estimates were based on the steady state relationship between glucose and glucose turnover or by compartmental analysis of labeled and unlabeled glucose dynamics after intravenous injection.

In contrast to previous studies, we failed to observe a positive y-intercept, i.e., "apparent" glucose uptake at zero glucose (21, 22). While the explanation for the positive intercept has been controversial (30), its existence was taken to reflect the saturation of uptake by the brain. While species differences may contribute to our failure to observe this intercept, another possible explanation stems from the methods by which R_d was quantified in the present study. Previous clamp studies in which the intercept was observed were performed in which exogenous glucose was unlabeled. This methodology has been found by us and others (19, 31) to be flawed, in that R_d (and HGO) are underestimated because of dilution of the plasma glucose pool with unlabeled glucose. Underestimation of R_d is especially severe under conditions of high glucose turnover. It is therefore possible that the presence of a positive intercept on the glucose:R_d curve may represent an artifact in the curve due to underestimation of R_d at high glucose, which would effectively "flatten out" the dose response curve. Consistent with this explanation are the results of Lund-Andersen (32), who observed no clear evidence for saturation of central nervous system glucose uptake at fasting glucose, with an apparent $K_m > 100$ mg/dl. Further studies are indeed warranted to more fully examine this possibility.

Despite high dose SRIF, we observed a slight increase in insulin during the hyperglycemic clamp (Table I), although levels remained below pre-SRIF concentrations. To quantify the effects of this increase on HGO and R_d, we compared our results to euglycemic insulin dose response studies performed in our laboratory using GINF "spiked" with labeled glucose (33, 34). This comparison indicated that during hyperglycemia, the observed decrement in HGO was four- to sixfold greater than that seen when comparable elevations in insulin were induced at euglycemia. The increase in R_d was nearly eightfold greater than at euglycemia. Furthermore, the decrement in FFA noted during hyperglycemic clamps was 2.4-fold greater than that seen during euglycemia, although control experiments described herein suggest a possible additional influence of time (see Results). Thus, we feel comfortable that the striking changes in HGO and R_d observed during hyperglycemic clamps represent the marked ability of hyperglycemia per se on glucose fluxes.

The hyperglycemia-mediated increase in R_d, which includes uptake by peripheral tissues and liver, is generally believed to occur by mass action, via an increase in intracellular glucose-6-phosphate (35), as well as by activation of key rate-limiting enzymes such as glucokinase and/or glycogen synthase (35, 36). Recently, however, evidence has emerged indicating GLUT4 translocation to the plasma membrane by glucose itself in skeletal muscle (37). Glucose disposal during normoinsulinemic hyperglycemia may also occur in splanchnic and hepatic tissues, but the analyses used in this study do not allow us to identify specific tissues involved in glucose's actions to stimulate uptake. However, the present study does confirm that glucose-stimulated R_d is a major contributor to glucose disappearance after a transient (i.e., IVGTT) or sustained (i.e., clamp) hyperglycemic stimulus, and that there are both uptake and glucose production components to glucose effectiveness.

The importance of glucose effectiveness to intravenous tolerance has been estimated from IVGTTs performed in dogs in the presence of a full-blown β-cell response (4). These previous results indicate that ~50% of the increase in R_d during injected glucose was due to glucose effectiveness. If we assume that glucose-stimulated glucose utilization (i.e., $GE_{IVGTT(uptake)}$) represents 72% of total glucose effectiveness, then the combined effects of glucose on HGO and R_d during the IVGTT may account for $0.50 \times 0.72 = 0.36$, or 36% of glucose normalization. This value in dogs is slightly lower than that observed by Kahn et al. (38), who reported that in normal subjects, nearly half of the variability in glucose tolerance could be explained by variability in glucose effectiveness (i.e., $r^2 = 0.49$). This difference may be due to species differences, or may reflect the importance of basal insulin on glucose effectiveness, since insulin was unintentionally underreplaced in the present study. Thus, these data indicate that glucose effectiveness contributes significantly to intravenous glucose tolerance even under normal, nondiabetic conditions.

Since both IVGTTs and multistep hyperglycemic clamps were performed on each animal, it is possible to compare glucose effectiveness derived from intravenous glucose injection to analogous measures obtained under steady state conditions. Parameter $GE_{IVGTT(total)}$ represents the increase in fractional net glucose disappearance that would be predicted from a given increase in plasma glucose, at fixed basal insulin. In this study, $GE_{IVGTT(total)} = 0.0298$ min^{-1} (Table VI); this implies that increasing the plasma glucose by 100 mg/dl, at basal insulin, will increase net glucose disappearance by 2.98 mg/min per dl of the glucose pool. When multiplied by the glucose distribution volume (33.2 dl; see Table V), $GE_{IVGTT(total)} = 0.986$ dl/min. This can be compared to $GE_{CLAMP(total)}$, which when multiplied by each animal's body weight (in kilograms), is expressed in similar units (deciliters per min). The clamp-derived measure of total glucose effectiveness is 1.155 dl/min, which is slightly, but not significantly greater than that obtained from the IVGTT. Similar comparisons can be made for R_d and HGO components; when expressed in similar units, the mean value of $GE_{(uptake)}$ (0.690±0.084 vs 0.866±0.162 dl/min) and $GE_{(HGO)}$ (0.297±0.081 vs 0.259±0.017 dl/min) were not different between the IVGTT and hyperglycemic clamp ($P = 0.38$ and 0.63, respectively). However, correlation of clamp-based versus IVGTT-based measures was minimal ($r = 0.22$). This is largely because of the relatively narrow range of glucose effectiveness observed in our sample of normal dogs. In fact, this r-value was similar to that obtained by simulation analysis. We assumed the two methods yield identical values of glucose effectiveness in any individual dog, and 10% random error (e.g., due to known day-to-day variability in glucose effectiveness [39]) was added; the maximum r-value possible was 0.24 [$n = 8$ simulations]). Thus, validation of glucose effectiveness remains to be performed, and will be aided by newly described agents which modulate glucose effectiveness in vivo (40).

It is also possible to compare $GE_{CLAMP(uptake)}$ calculated in this study with estimates obtained in the literature. By defining this parameter as the change in R_d for a given increment in glucose, at fixed basal insulin, this working definition can be applied to the most widely used clamp-based index of glucose action, non–insulin-mediated glucose uptake (41–43), defined as R_d during somatostatin-induced insulinopenia. Baron and coworkers (41) report that in humans, when glucose was raised from 88 to 220 mg/dl at "zero" insulin in normal subjects, R_d

rose from 128 to 213 mg/min. Thus, clamp-based $GE_{(uptake)}$ = 0.644 dl/min for non–insulin-mediated glucose uptake data obtained at zero insulin. This value is slightly lower than that obtained from our clamps (0.866 dl/min), and consistent with the fact that the current study was performed at near-basal insulin.

Given the preponderance of studies in which models of glucose kinetics have been applied to the IVGTT (15, 17, 18, 44–46), it is valid to question the contribution of the present model and its application in this study. The uniqueness of the present study lies not in the model per se, but in its application to an experimental protocol designed solely to quantify glucose effectiveness and its component factors. Unlike previous estimates of glucose effectiveness from the IVGTT (2, 10), we blocked the insulin response with SRIF to create a simpler glucose dynamic in which changes in disappearance depend solely on glucose itself. The optimal model could then be designed without needing to account for insulin action, thereby avoiding any potential interference of insulin on model choice or estimation of glucose effectiveness (7). Finally, adding tracer to the glucose bolus enabled us to assess the discrete actions of glucose on uptake and production. With a specific, well-defined experimental protocol in hand, we determined that the two-compartment model (Fig. 1) was the best representation of labeled glucose dynamics after injection, based on multiple goodness-of-fit criteria (see Appendix). The chosen model is structurally similar to those previously proposed (17, 18, 46, 47).

There are two reasons to suggest that values of glucose effectiveness and its component parts are accurate in the present study. First, we have previously performed SRIF-suppressed IVGTTs in normal dogs to measure glucose effectiveness directly (3), and the results compared with values obtained by minimal model analysis (since tracer was not injected, only total S_G was estimated). From those studies, glucose effectiveness measured directly was 0.025 min^{-1}, and minimal model estimates obtained from standard and tolbutamide-modified IVGTTs were 0.033 and 0.028 min^{-1} (3). Thus, all three measures obtained in dogs (direct estimate in absence of secreted insulin, and two minimal model parameters) were remarkably similar to the value of $GE_{IVGTT(total)}$ obtained from the presumably more accurate two-compartment model approach used in the present study in dogs (0.0298 min^{-1}; Table VI). Finally, values of glucose effectiveness calculated from hyperglycemic clamps in dogs indicate that the relative contribution of $GE_{(uptake)}$ and $GE_{(HGO)}$ is remarkably similar to that obtained from two-compartmental analysis of the IVGTT with tracer injection during SRIF. This evidence suggests that certain prior attempts to quantify glucose effectiveness and its uptake component may have to be reexamined to further clarify differences in results. It appears that the actual value of glucose effectiveness in dogs is $\sim$ 0.030 min^{-1}, which validates many studies using the minimal model (4).

Two known IVGTT approaches to study glucose effectiveness have been widely published. The usual approach to estimation of glucose effectiveness is the minimal model, applied to the IVGTT with unlabeled glucose injection (2, 3, 48). (Insulin secretagogues have been introduced at 20 min after glucose injection to improve accuracy of parameter estimation [49]). This approach was designed to determine overall S_G, with both uptake and HGO components, since tracer is not injected to segregate these effects. The second approach is the use of modified minimal models, applied to IVGTTs in which labeled glucose is injected along with cold glucose (10, 50, 51). This latter approach is used to determine both total glucose effectiveness and its uptake component. Both of these IVGTT protocols are characterized by an unrestrained glucose-stimulated insulin response. Glucose effectiveness quantified in the present study can be compared to glucose effectiveness calculated from these two approaches.

Cobelli et al. (10) have proposed a protocol using the labeled IVGTT—glucose plus tracer (radioactive or stable) injection, with a normal insulin response—combined with modified minimal model analysis to estimate both total glucose effectiveness, and the uptake component, termed S_G*. They have reported that S_G* was 0.0092 min^{-1} in normal subjects, which is only 45% of the $GE_{IVGTT(uptake)}$ reported here (0.0206 min^{-1}; Table VII). From the same previous study, total S_G was estimated at 0.042 min^{-1}, which is 41% greater than $GE_{IVGTT(total)}$ obtained in the present study (0.0298 min^{-1}). Based upon the previous results, data of Cobelli et al. would suggest that glucose's effect to suppress HGO would dominate overall glucose effectiveness, as S_G* represents only 31% of total S_G. (More recently, this group reported lower values of S_G* and S_G in normal subjects [0.0080 and 0.0255 min^{-1}]; however, the contribution of the uptake component remains 31% [8]). It is pos-

Table VII. Comparison of Glucose Effectiveness Estimates between Two-Compartment Glucose Distribution Analysis and the Minimal Model (Single Glucose Compartment)

IVGTT Protocol		No. glucose compartments	Glucose effectiveness estimates (min^{-1})*		Reference
Glucose data analyzed	Insulin response?		Overall GE	GE (R_d only)	
Labeled and unlabeled	No	Two	0.0298±0.0022	0.0206±0.0014	Current study
Labeled and unlabeled	Yes	One‡	0.042±0.009	0.0092±0.0009	(10)
Labeled and unlabeled	Yes	One‡	0.0255±0.0021	0.0080±0.0012	(8)
Unlabeled	Yes	One	0.033±0.004	NA§	(3)
Unlabeled	Yes	One	0.028±0.003	NA	(3)‖

‡One-compartment model represents the minimal model, modified in references 8 and 10 to analyze both labeled and unlabeled glucose. ‖Data obtained from glucose + tolbutamide IVGTT. *All glucose effectiveness values derived from the minimal model were adjusted for differences in distribution volume to permit comparison between one- and two-compartment representations (see Discussion). There was no statistical difference between GE parameters representing combined actions of glucose on HGO and R_d (overall GE). However, glucose effectiveness for glucose uptake from Cobelli et al. (=S_G*; [8, 10]) was significantly lower than $GE_{IVGTT(uptake)}$ obtained from the present study ($P < 0.005$). §Not available. Estimates of the uptake component of glucose effectiveness cannot be obtained without labeled glucose data.

sible that a single compartment of glucose kinetics as used by Cobelli et al. is insufficient to fully account for both cold and labeled glucose kinetics during the IVGTT. The possible influence of a full insulin profile, which is elicited in the Cobelli approach but not in the SRIF-suppressed IVGTTs of the present study, may also contribute to the disparate answers between the two approaches. The advantage of the present approach is that glucose effectiveness can be determined in the absence of the potentially confounding effect of dynamic insulin. Without insulin, it was clear that the dominant effect of glucose itself was on glucose uptake ($\sim$ 70%), with only a lesser hepatic component ($\sim$ 30%).

In conclusion, this study provides the first quantitative analysis of glucose effectiveness and the relative contributions of glucose-mediated stimulation of glucose disposal and suppression of endogenous glucose production to overall glucose effectiveness. By using a two-compartment representation of glucose kinetics, we observed that the dominant action of glucose is to stimulate R_d ($GE_{(uptake)}$ = 72% of total glucose effectiveness). Interestingly, while glucose's effect to inhibit production ($GE_{(HGO)}$) is quantitatively smaller than $GE_{(uptake)}$ (0.0092 vs 0.0206 min^{-1}, respectively), it is highly variable in normal animals and may indeed exceed glucose's actions on utilization. Thus, it is important to recognize that glucose effectiveness is not insulin-independent glucose uptake alone, but rather includes a significant autoregulatory action to suppress endogenous glucose supply. Whether the relative contributions of uptake and production, or the tissues involved in these processes, may vary in pathologic states such as diabetes remains to be investigated.

Appendix

Determination of optimal model structure. To determine the optimal model, we sought to develop a model that was structurally simple enough for precise parameter identification through experiments, yet of sufficient complexity to explain experiment results without significant bias. In this study, we determined the minimal number of compartments that were necessary to describe both unlabeled and labeled glucose dynamics when the normal insulin secretory response was suppressed by SRIF. For linear compartmental models, the solutions are well-defined. Generally speaking, the solution to a model of *n* number of compartments will be a linear combination of *n* exponential terms (16, 52).

We compared one, two, and three exponential fits to the labeled glucose data from IVGTTs performed in each of eight dogs, the kinetics of which are determined by R_d alone. Adequacy of model fits was determined by residual time course and five goodness-of-fit indices (53): unweighted or weighted residual sum-of-squares (SSQ and SSQ_w), weighted Akaike Information Criterion (AIC_w), and unweighted or weighted mean percent fractional standard deviation (mean %FSD and $\%FSD_w$).

The average model fits and residuals of the fits are shown in Fig. A1. Individual model fits for each dog reveals similar trends shown in Fig. A1 (data not shown). The monoexponential function fit poorly to the tracer dynamic over the entire time scale, as evidenced by significant bias in the time course of residuals. In contrast, no significant bias was found in either two or three exponential fits. Statistical comparison of goodness-of-fit indices are presented in Table AI. Significant improvement of SSQ and AIC was observed when the exponential number increased from one to two; the SSQ was reduced 15-fold (22.9 to 1.6), SSQ_w decreased by 90%, and AIC_w reduced 39%. No significant improvement in any index was found by increasing the number of exponentials from two to three. Finally, mean %FSD were satisfactory for both one and two exponential fits (< 10% for both), but were unacceptably large with the fit to three exponentials (> 10,000%).

Thus, the overall precision of parameter estimation for fitting tracer data to three exponentials was inadequate in comparison to either one or two exponential fit. We concluded that with all factors considered, the two-exponential function is the

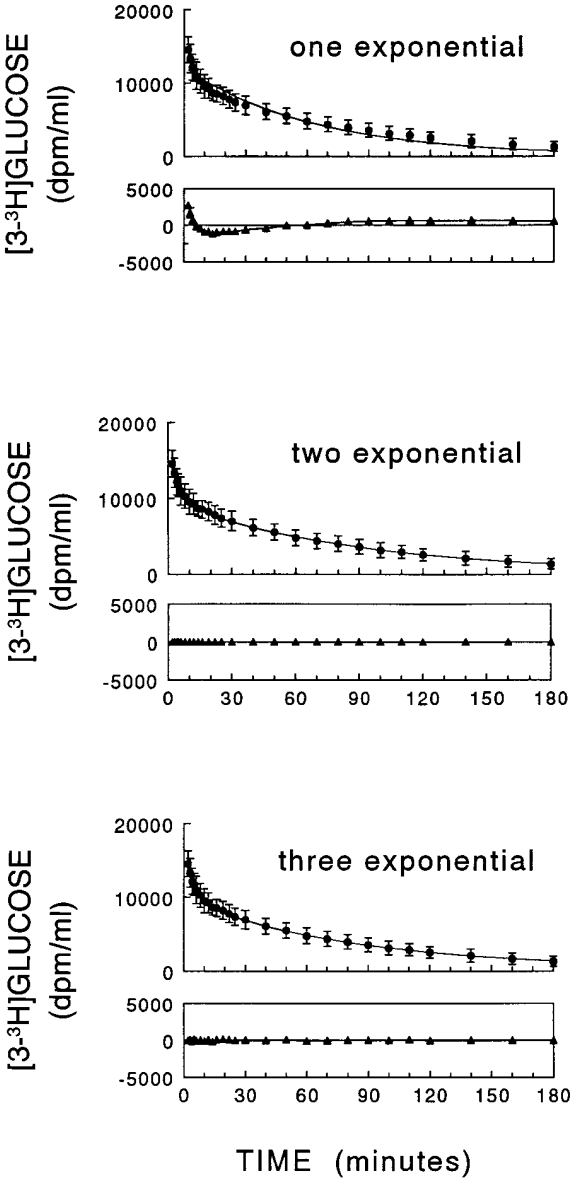

Figure A1. Exponential analysis of labeled glucose data to determine the optimal degree of model complexity. Tracer data from each of eight experiments were fit to one-, two-, and three-compartment models. Average model fit, with residuals, are shown for each exponential fit. Based upon multiple goodness-of-fit criteria, the two-compartment representation was deemed optimal for estimation of glucose effectiveness from available data.

Table AI. Goodness-of-Fit Indices for Various Model Fits

Model	SSQ (10^6)	SSQ_w	AIC_w	Mean %FSD	Mean $\%FSD_w$
1 exponential	22.9±3.0	159.54±18.2	134.47±3.39	5.66±0.14	3.24±0.17
2 exponential	1.57±0.50	19.77±3.74	82.49±4.74	6.68±1.59	9.26±2.62
3 exponential	1.34±0.52	16.16±2.70	82.18±3.86	> 10,000	> 10,000

Data are mean±SE (n = 8 for each model fit). SSQ represents the residual sum-of-squares, and AIC denotes the Akaike information criterion. Mean %FSD is the fractional standard deviation for any given parameter. Subscript w indicates that inverse variance weighting has been applied for the model fit.

best representation to describe labeled glucose data after injection.

Finally, in the selected two-compartment model shown in Fig. 1, HGO is defined as a linear function of plasma glucose concentration (Eq. 3). While this relationship has been confirmed by the glucose clamp results presented in this study, assumption of this linearity under dynamic conditions such as during the IVGTT remain to be verified by further investigation.

Assumptions required for identifiability. The two-compartment model in Fig. 1 is a priori unidentifiable by the plasma glucose and tracer concentration profile alone. For the present analysis, we assumed that at basal insulin, all glucose disappearance occurs from the first compartment, i.e., $k_{02} = 0$ (17, 18). We examined the possible influence of this assumption on our assessment of the relative contribution of glucose's effects on uptake and production to glucose effectiveness. We tested two alternative assumptions in the calculation of relative contributions of uptake and HGO to overall glucose effectiveness: (*a*) that $k_{02} = k_{01}$ (17, 44), and (*b*) that $k_{02}/k_{01} \sim 0.3$, i.e., that uptake from the second compartment is about one-third of glucose uptake from compartment 1 at basal insulin (15). The k_{02}/k_{01} ratio was also varied evenly from 0 to 1.2 to cover the assumptions listed above.

Relative contribution for each dog under various assumptions were calculated, and are shown in Fig. A2. We found that the contribution of $GE_{IVGTT(uptake)}$ differed minimally (1.3% and 3.0%) between the model under our $k_{02} = 0$ assumption, and either the 1:3 partition or the $k_{02} = k_{01}$ assumption. Although initially surprising, we recognized that since $GE_{IVGTT(uptake)}$ and $GE_{IVGTT(HGO)}$ under these assumptions were determined by the identical labeled and unlabeled plasma glucose dynamics, the combination of all parameters from the model (k_{01}, k_{02}, k_{12}, k_{21}, k_L, and V_1), under any assumption, must fit the same glucose data. Hence, if $GE_{IVGTT(uptake)}$ and $GE_{IVGTT(HGO)}$ from our two-compartment model adequately characterize both labeled and unlabeled glucose dynamics, their relative contributions should not vary when they are determined from the same glucose and tracer profiles. Our analysis confirmed that the relative contribution of uptake and HGO to overall glucose effectiveness was determined only by the labeled and unlabeled glucose dynamics and was not affected by the k_{02} assumption.

Acknowledgments

The authors express their gratitude to the technical assistance given by Elza Demirchyan and Lena Minassian for performance of assays. Thanks are also extended to Donna Moore for her caring treatment of our animals, as well as expert surgical assistance.

This work was supported by grants from the National Institutes of Health (NIH) to R.N. Bergman (DK29867 and DK27619) and M. Ader (AG00544). R.N. Bergman is also supported by the Salerni Collegium of the University of Southern California. T.-C. Ni was supported by the National Heart, Lung, and Blood Institutes of the NIH (HL-47890).

References

1. Fuller, J.H., M.J. Shipley, G. Rose, R.J. Jarrett, and H. Keen. 1980. Coronary heart-disease risk and impaired glucose tolerance: the Whitehall study.

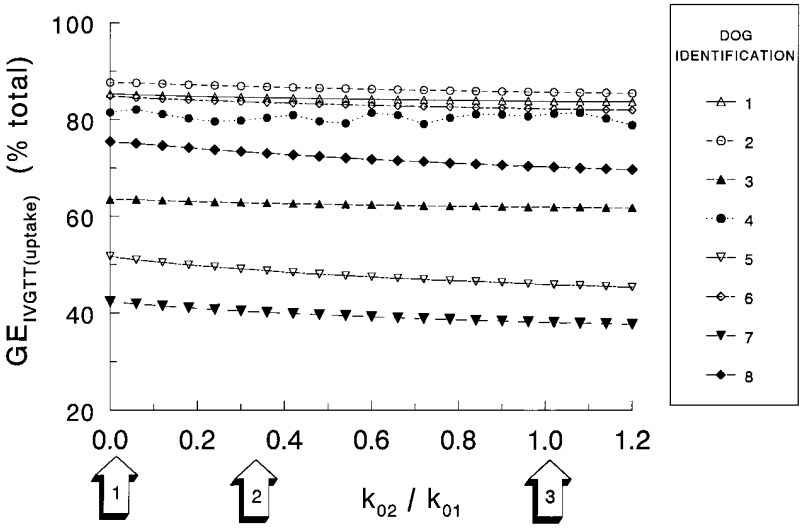

Figure A2. Effect of k_{02} assumptions on calculation of relative contribution of $GE_{IVGTT(uptake)}$ to overall glucose effectiveness. Two-compartment model analysis was performed for each dog using different k_{02}/k_{01} ratios, which were varied between 0 and 1.2 (see text). Arrows on x-axis indicate three specific assumptions tested: (*a*) that $k_{02} = 0$ (17, 18); (*b*) the assumption of 1:3 partitioning between uptake from two compartments (15); (*c*) that $k_{01} = k_{02}$ (17, 44).

Lancet. i:1373–1376.

2. Bergman, R.N., Y.Z. Ider, C.R. Bowden, and C. Cobelli. 1979. Quantitative estimation of insulin sensitivity. *Am. J. Physiol.* 236:E667–E677.

3. Ader, M., G. Pacini, Y.J. Yang, and R.N. Bergman. 1985. Importance of glucose per se to intravenous glucose tolerance: comparison of the minimal model prediction with direct measurements. *Diabetes.* 34:1092–1103.

4. Bergman, R.N., T.-C. Ni, and M. Ader. 1996. Glucose effectiveness. *In* Clinical Research in Diabetes. B. Draznin and R. A. Rizza, editors. Humana Press, Totowa, NJ. pp. 81–100.

5. Martin, B.C., J.H. Warram, A.S. Krolewski, R.N. Bergman, J.S. Soeldner, and C.R. Kahn. 1992. Role of glucose and insulin resistance in development of type 2 diabetes mellitus: results of a 25-year follow-up study. *Lancet.* 340:925–929.

6. Quon, M.J., C. Cochran, S.I. Taylor, and R.C. Eastman. 1994. Non–insulin-mediated glucose disappearance in subjects with IDDM: discordance between experimental results and minimal model analysis. *Diabetes.* 43:890–896.

7. Finegood, D.T., and D. Tzur. 1996. Reduced glucose effectiveness associated with reduced insulin release: an artifact of the minimal-model method. *Am. J. Physiol.* 271:E485–495.

8. Vicini, P., A. Avogaro, A. Valerio, A. Caumo, and C. Cobelli. 1996. Glucose effectiveness, clearance rate and peripheral insulin sensitivity are impaired in NIDDM subjects: a hot IVGTT minimal model study. *Diabetes.* 45 (Suppl. 2):100*a*. (Abstr.)

9. Christopher, M.J., C. Rantzau, G.M. Ward, and F.P. Alford. 1995. Insulinopenia and hyperglycemia influence the in vivo partitioning of GE and SI. *Am. J. Physiol.* 268:E410–E421.

10. Cobelli, C., G. Pacini, G. Toffolo, and L. Sacca. 1986. Estimation of insulin sensitivity and glucose clearance from minimal model: new insights from labeled IVGTT. *Am. J. Physiol.* 250:E591–E598.

11. Ader, M., and R.N. Bergman. 1990. Peripheral effects of insulin dominate suppression of fasting hepatic glucose production. *Am. J. Physiol.* 258: E1020–E1032.

12. Andersen, L., B. Dinesen, P.N. Jorgensen, F. Poulsen, and M.E. Roder. 1993. Enzyme immunoassay for intact human insulin in serum or plasma. *Clin. Chem.* 39:578–582.

13. Somogyi, M. 1945. Determination of blood sugar. *J. Biol. Chem.* 160:69–73.

14. Jacquez, J.A. 1992. Theory of production rate calculations in steady and non-steady states and its application to glucose metabolism. *Am. J. Physiol.* 262:E779–E790. (Editorial).

15. Cobelli, C., G. Toffolo, and E. Ferrannini. 1984. A model of glucose kinetics and their control by insulin: compartmental and noncompartmental approaches. *Mathematical Biosciences.* 72:291–315.

16. Norwich, K.H. 1977. Molecular Dynamics in Biosystems: The Kinetics of Tracers in Intact Organisms. Pergamon Press, Oxford. 405 pp.

17. Radziuk, J., K.H. Norwich, and M. Vranic. 1978. Experimental validation of measurements of glucose turnover in non–steady state. *Am. J. Physiol.* 234:E84–E93.

18. Katz, J., A. Dunn, M. Chenoweth, and S. Golden. 1974. Determination of synthesis, recycling and body mass of glucose in rats and rabbits in vivo with ^{3}H- and ^{14}C-labeled glucose. *Biochem. J.* 142:171–183.

19. Bergman, R.N., D.T. Finegood, and M. Ader. 1985. Assessment of insulin sensitivity in vivo. *Endocr. Rev.* 6:45–86.

20. Hendrick, G.K., R.T. Frizzell, and A.D. Cherrington. 1987. Effect of somatostatin on nonesterified fatty acid levels modifies glucose homeostasis during fasting. *Am. J. Physiol.* 253:E443–E452.

21. Best, J.D., G.J. Taborsky, Jr., J.B. Halter, and D. Porte, Jr. 1981. Glucose disposal is not proportional to plasma glucose level in man. *Diabetes.* 30: 847–850.

22. Verdonk, C.A., R.A. Rizza, and J.E. Gerich. 1981. Effects of plasma glucose concentration on glucose utilization and glucose clearance in normal man. *Diabetes.* 30:535–537.

23. Bergman, R.N. 1989. Toward physiological understanding of glucose tolerance: minimal-model approach. *Diabetes.* 38:1512–1527. (Lilly Lecture.)

24. Welch, S., S.S.P. Gebhart, R.N. Bergman, and L.S. Phillips. 1990. Minimal model analysis of intravenous glucose tolerance test-derived insulin sensitivity in diabetic subjects. *J. Clin. Endocrinol. Metab.* 71:1508–1518.

25. Henriksen, J.E., F. Alford, A. Handberg, A. Vaag, G.M. Ward, A. Kalfas, and H. Beck-Nielsen. 1994. Increased glucose effectiveness in normoglycemic but insulin-resistant relatives of patients with non-insulin-dependent diabetes mellitus. *J. Clin. Invest.* 94:1196–1204.

26. Porte, D., Jr. 1991. B-cells in type II diabetes mellitus. *Diabetes.* 40:166–180. (Banting Lecture.)

27. Alzaid, A.A., S.F. Dinneen, D.J. Turk, A. Caumo, C. Cobelli, and R.A. Rizza. 1994. Assessment of insulin action and glucose effectiveness in diabetic and nondiabetic humans. *J. Clin. Invest.* 94:2341–2348.

28. Bonadonna, R.C., S. Del Prato, M.P. Saccomani, E. Bonora, G. Gulli, E. Ferrannini, D. Bier, C. Cobelli, and R.A. DeFronzo. 1993. Transmembrane glucose transport in skeletal muscle of patients with non-insulin-dependent diabetes. *J. Clin. Invest.* 92:486–494.

29. Ader, M., and T.-C. Ni. 1996. Glucose effectiveness accounts for 42% of glucose disposal after oral glucose. *Diabetes.* 45 (Suppl. 2):100*a*. (Abstr.)

30. Gottesman, I., L. Mandarino, and J. Gerich. 1983. Estimation and kinetic analysis of insulin-independent glucose uptake in human subjects. *Am. J. Physiol.* 224:E632–E635.

31. Vranic, M., P. Fono, N. Kovacevic, and B. J. Lin. 1971. Glucose kinetics and fatty acids in dogs on matched insulin infusion after glucose load. *Metab. Clin. Exp.* 20:954–967.

32. Lund-Andersen, H. 1979. Transport of glucose from blood to brain. *Physiol. Rev.* 59:305–352.

33. Rebrin, K., G.M. Steil, L. Getty, and R.N. Bergman. 1995. Free fatty acid as a link in the regulation of hepatic glucose output by peripheral insulin. *Diabetes.* 44:1038–1045.

34. Bradley, D.C., R.A. Poulin, and R.N. Bergman. 1992. Dynamics of hepatic and peripheral insulin effects suggest common rate-limiting step in vivo. *Diabetes.* 42:296–306.

35. Farrace, S., and L. Rossetti. 1992. Hyperglycemia markedly enhances skeletal muscle glycogen synthase activity in diabetic, but not in normal conscious rats. *Diabetes.* 41:1453–1463.

36. Kruszynska, Y.T., P.D. Home, and K.G.M.M. Alberti. 1986. In vivo regulation of liver and skeletal muscle glycogen synthase activity by glucose and insulin. *Diabetes.* 35:662–667.

37. Galante, P., L. Mosthaf, M. Kellerer, L. Berti, S. Tippmer, B. Bossenmaier, T. Fujiwara, A. Okuno, H. Horikoshi, and H.U. Haring. 1995. Acute hyperglycemia provides an insulin-independent inducer for GLUT4 translocation in C_2C_{12} myotubes and rat skeletal muscle. *Diabetes.* 44:646–651.

38. Kahn, S.E., R.L. Prigeon, D.K. McCulloch, E.J. Boyko, R.N. Bergman, M.W. Schwartz, J.L. Neifing, W.K. Ward, J.C. Beard, J.P. Palmer, and D. Porte, Jr. 1994. The contribution of insulin-dependent and insulin-independent glucose uptake to intravenous glucose tolerance in healthy human subjects. *Diabetes.* 43:587–592.

39. Steil, G.M., J. Murray, R.N. Bergman, and T.A. Buchanan. 1994. Repeatability of insulin sensitivity and glucose effectiveness from the minimal model: implications for study design. *Diabetes.* 43:1365–1371.

40. Hobbs, C.J., R.E. Jones, and S.R. Plymate. 1996. Nandrolone, a 19-nortestosterone, enhances insulin-independent glucose uptake in normal men. *J. Clin. Endocrinol. Metab.* 81:1582–1585.

41. Baron, A.D., G. Brechtel, P. Wallace, and S.V. Edelman. 1988. Rates and tissue sites of non-insulin- and insulin-mediated glucose uptake in humans. *Am. J. Physiol.* 255:E769–E774.

42. Edelman, S.V., M. Laakso, P. Wallace, G. Brechtel, J.M. Olefsky, and A.D. Baron. 1990. Kinetics of insulin-mediated and non-insulin-mediated glucose uptake in humans. *Diabetes.* 39:955–964.

43. Baron, A.D., O.G. Kolterman, J. Bell, L.J. Mandarino, and J.M. Olefsky. 1985. Rates of non–insulin-mediated glucose uptake are elevated in type II diabetic subjects. *J. Clin. Invest.* 76:1782–1788.

44. Raman, M., J. Radziuk, and G.J. Hetenyi. 1990. Distribution and kinetics of glucose in rat analyzed by noncompartmental and compartmental analysis. *Am. J. Physiol.* 259:E292–E303.

45. Insel, P.A., J.E. Liljenquist, J.D. Tobin, R.S. Sherwin, P. Watkins, R. Andres, and M. Berman. 1975. Insulin control of glucose metabolism in man. *J. Clin. Invest.* 55:1057–1066.

46. Atkins, G. 1980. A new technique for maintaining and monitoring conscious, stress-free rabbits in a steady state: its use in the determination of glucose kinetics. *Quart. J. Exp. Physiol.* 65:63–75.

47. Caumo, A., and C. Cobelli. 1993. Hepatic glucose production during the labeled IVGTT: estimation by deconvolution with a new minimal model. *Am. J. Physiol.* 264:E829–E841.

48. Osei, K., and D.P. Schuster. 1995. Metabolic characteristics of African descendants: a comparative study of African-Americans and Ghanaian immigrants using minimal model analysis. *Diabetologia.* 38:1103–1109.

49. Yang, Y.J., J.H. Youn, and R.N. Bergman. 1987. Modified protocols improve insulin sensitivity estimation using the minimal model. *Am. J. Physiol.* 253:E595–E602.

50. Avogaro, A., J.D. Bristow, D.M. Bier, C. Cobelli, and G. Toffolo. 1989. Stable-label intravenous glucose tolerance test minimal model. *Diabetes.* 38: 1048–1055.

51. Caumo, A., A. Giacca, M. Morgese, G. Pozza, P. Micossi, and C. Cobelli. 1991. Minimal models of glucose disappearance: lessons from the labeled IVGTT. *Diab. Med.* 8:822–832.

52. Jacquez, J.A. 1985. Compartmental Analysis in Biology and Medicine. University of Michigan Press, Ann Arbor. 560 pp.

53. Watanabe, R.M., J. Lovejoy, G.M. Steil, M. DiGirolamo, and R.N. Bergman. 1995. Insulin sensitivity accounts for glucose and lactate kinetics after intravenous glucose. *Diabetes.* 44:954–962.